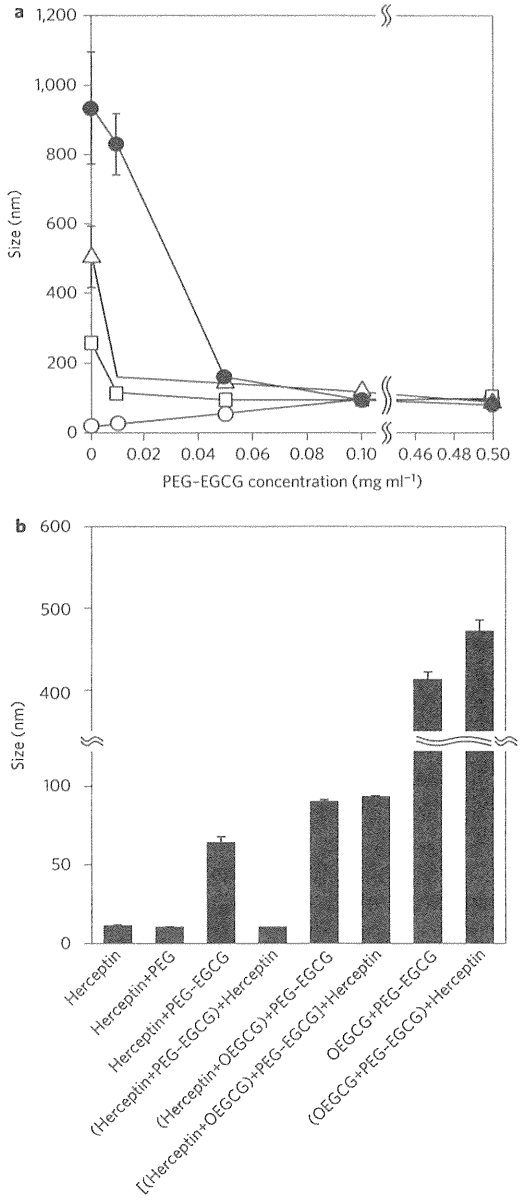

Figure 3 | Core-shell MNC formation. a, Complex size obtained when PEG-EGCG of various concentrations was added to pre-formed Herceptin/OEGCG complexes (OEGCG = 0.09 μg ml^{-1}, open circles; 3 μg ml^{-1}, open squares; 6 μg ml^{-1}, open triangles; 12 μg ml^{-1}, filled circles). PEG-EGCG assembled around Herceptin/OEGCG complexes of varied sizes, yielding uniformly sized complexes at a critical PEG-EGCG concentration. The uniform size remained constant, regardless of any further increase in PEG-EGCG concentration (n = 3, mean ± s.d.). **b**, Complexes formed with various compositions and adding sequences. The sequential two-step self-assembly (the assembly of OEGCG with Herceptin followed by PEG-EGCG assembly around the Herceptin/OEGCG complex) was necessary to construct the stable and spatially ordered MNC, which showed no change in size with the post-addition of Herceptin (n = 3, mean ± s.d.).

We also studied the activities of the proteins during the complexation and dissociation process. Ideally, the complexes should stably preserve the proteins from activity loss, degradation and interaction with other molecules during delivery, but exert their therapeutic activities at the sites of delivery. Figure 2c shows that the activities of various proteins were restrained by complexation with OEGCG. However, the activities were fully restored when the complexes were dissociated. Accordingly, complexation of the proteins could protect the proteins from potential environmental damage and undesirable side effects during delivery, and their temporarily masked bioactivity could be reestablished on dissociation of the complexes when delivered/accumulated.

To construct the outer shell surrounding the core complex, PEG–EGCG was added to the pre-formed Herceptin/OEGCG complexes. When PEG–EGCG was added in increasing amounts to Herceptin/OEGCG complexes of various sizes, complexes were formed with a uniform size that remained constant, despite further increases in PEG–EGCG concentration (Fig. 3a). TEM images show that, as the OEGCG concentration increases, the increase in the average size of Herceptin/OEGCG complexes is due to an increasing number of pre-existing Herceptin/OEGCG complexes complexing with one another, rather than an increase in the diameter of pre-existing complexes (Supplementary Fig. 5). This phenomenon has been observed in the mechanism for polyphenol/protein complexation, in which pre-existing complexes associate by bridging through polyphenols when the polyphenol concentration is increased[28]. The inter-complex association between Herceptin/OEGCG complexes was probably dissociated by PEG–EGCG due to hydrophobic competition with the EGCG moieties of PEG–EGCG. Subsequently, PEG–EGCG assembled around the Herceptin/OEGCG complex at a critical PEG–EGCG concentration, yielding uniformly sized complexes with favourably balanced interaction energy. The constant complex size above the critical PEG–EGCG concentration could be due to repulsion by the PEG outer shell resisting further assembly.

We also found that both the composition and the sequence of addition affected the construction of the MNCs (Fig. 3b). In the absence of OEGCG, PEG–EGCG still formed MNCs with Herceptin, whereas PEG did not assemble with Herceptin. However, the Herceptin/PEG–EGCG complex was dissociated by the post-addition of Herceptin. In contrast, MNCs formed by the sequential two-step self-assemblies, that is, the assembly of OEGCG with Herceptin, followed by PEG–EGCG assembly around the Herceptin/OEGCG complex, showed no change in size, despite the post-addition of Herceptin. OEGCG might have played an important role in stabilizing the complex structure by producing a more crosslinked and hydrophobic core that strengthened binding with PEG–EGCG, while the stably formed PEG shell isolated the core from access by subsequently added proteins. When PEG–EGCG was added directly to OEGCG without the pre-complexation of OEGCG and Herceptin, huge complexes were obtained and the size further increased with the post-addition of Herceptin. The PEG–EGCG and OEGCG were considered to form a complex by hydrogen bonding between oxygen through an ether linkage of the PEG chain and the phenolic hydroxyl group of the OEGCG[29], which was not reversible with the post-addition of Herceptin. Accordingly, pre-complexation of Herceptin/OEGCG (OEGCG chains were considered to be mostly folded) was necessary to construct the stable and spatially ordered MNCs. This micellar structure was also supported by ζ-potential analysis, which showed a significant decrease in the surface charge of the Herceptin/OEGCG complex after adding PEG–EGCG, suggesting that the PEG chains covered the core complex surface (Supplementary Fig. 6).

The MNCs retained their integrity and demonstrated good stability in the presence of serum at 37 °C for 15 days, without any change in size (Supplementary Fig. 7). Furthermore, they did not undergo any size reduction following a 1000-fold dilution, showing excellent stability as a function of suspension dilution, as would occur *in vivo* (Supplementary Fig. 8). Moreover, the

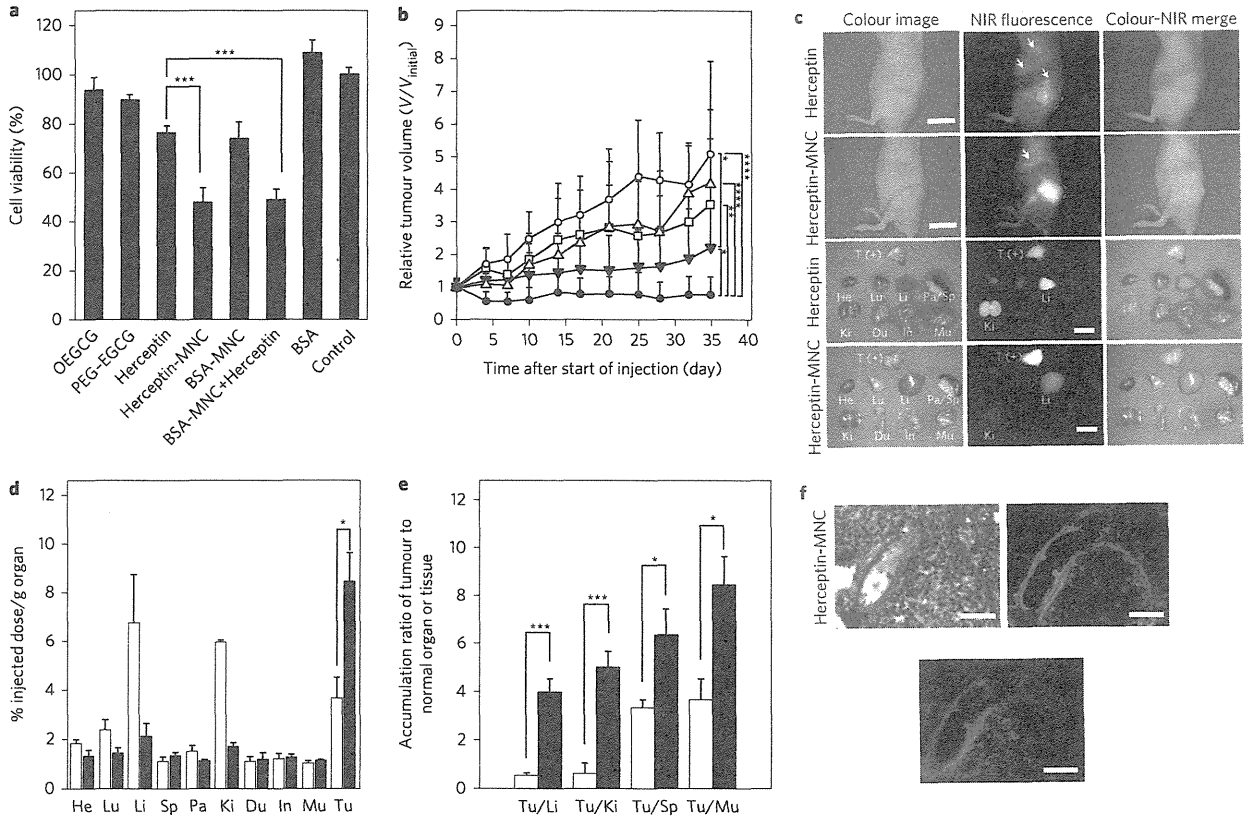

Figure 4 | Anticancer effect and biodistribution of the MNCs. a, The growth inhibitory effects of Herceptin, Herceptin-MNC, BSA-MNC (drug-free carrier), a mixture of BSA-MNC and Herceptin, BSA, OEGCG and PEG-EGCG (carrier components) on BT-474 cells (human breast cancer cell line). Note that the control group are untreated cells. See Methods for a detailed description. Herceptin-MNC showed a higher cancer cell growth inhibitory effect than free Herceptin as a result of synergism of the inhibitory effects of the carrier and Herceptin ($n = 5$, mean ± s.d., $^{***}P < 0.001$). **b**, Anticancer effect on BT-474-xenografted nude mouse model. PBS (vehicle control, open circles), BSA-MNC (open triangles), Herceptin (2.5 mg kg^{-1}, open squares), sequential injection of BSA-MNC and Herceptin (filled inverted triangles) and Herceptin-MNC (filled circles) in the same formulations as those used in **a**. Herceptin-MNC showed a significantly higher anticancer effect than sequentially injected BSA-MNC and Herceptin, as well as free Herceptin ($n = 12$, mean ± s.d., $^{*}P < 0.05$, $^{**}P < 0.01$, $^{****}P < 0.0001$). **c**, Real-time intraoperative tumour detection and NIR fluorescence image-guided resection at 24 h post-injection. Arrows indicate non-specific uptake (liver, kidneys, intestine). The red dashed circle delineates the region of interest. T (+), positive tumour; He, heart; Lu, lung; Li, liver; Pa, pancreas; Sp, spleen; Ki, kidneys; Du, duodenum; In, intestine; Mu, muscle. Scale bars, 1 cm. **d**, Biodistribution of Herceptin (open bars) and Herceptin-MNC (filled bars) in major organs measured 24 h post-injection. Herceptin-MNC exhibited a 2.3-fold higher accumulation in tumour (Tu) and 0.3-, 0.3- and 0.6-fold lower accumulation in liver, kidney and lung, respectively, compared with free Herceptin at 24 h post-injection ($n = 5$, mean ± s.d., $^{*}P < 0.05$). **e**, Tumour-to-background (normal organ or tissue) ratio for Herceptin (open bars) and Herceptin-MNC (filled bars) at 24 h post-injection. Herceptin-MNC showed improved tumour selectivity over the surrounding normal organs or tissues, compared with free Herceptin ($n = 5$, mean ± s.d., $^{*}P < 0.05$, $^{***}P < 0.001$). **f**, Haematoxylin and eosin staining (top left), targeted NIR fluorescence (top right, pseudocoloured in lime green), and immunofluorescence staining (bottom, stained with Her2 primary antibody and Alexa Fluor 680 labelled secondary antibody, pseudocoloured in red) images of BT-474 xenograft tumour at 24 h post-injection. Herceptin-MNCs were observed throughout the extravascular space, consistent with localization of overexpressed HER2/neu receptors on the tumour, and suggesting extravasation and deep tumour penetration of Herceptin-MNC. Scale bars, 100 μm. All NIR fluorescence images have identical exposure times and normalization.

fluorescence-labelled protein-loaded MNCs showed a much slower increase in fluorescence intensity (resulting from degradation of the fluorescence-labelled protein in the presence of protease) than free protein. This demonstrated that the protein was safely protected from proteolysis by this MNC system (Supplementary Fig. 9).

The anticancer effect of the Herceptin-loaded MNCs was explored *in vitro* and *in vivo* and compared to that of free Herceptin (Fig. 4). The cancer cell growth inhibitory effect was observed on BT-474 (HER2-overexpressing human breast cancer cell line) after treatment with free Herceptin, Herceptin-loaded micellar nanocomplex (Herceptin–MNC), BSA-loaded micellar nanocomplex (BSA–MNC) (that is, drug-free carrier), a mixture of BSA–MNC and Herceptin, and an equivalent amount of each carrier component (OEGCG and PEG–EGCG) (Fig. 4a; see Methods). BSA–MNC had a cancer cell growth inhibitory effect due to the anticancer effect of OEGCG and PEG–EGCG, whereas BSA alone had no effect. Notably, Herceptin–MNC showed a higher inhibitory effect than free Herceptin as a result of synergism of the inhibitory effects of the carrier and Herceptin (with a combination index (CI) of 0.93) (Supplementary Section 10). The greater inhibitory effect of Herceptin–MNC was also observed on other HER2-overexpressing human cancer cells (SKBR-3 and SKOV-3), but no growth inhibitory effect was seen on normal cells (MCF-10A and HMEC) (Supplementary Fig. 10). Because the MNCs were formed via a hydrophobic interaction and would be dissociated by hydrophobic competition with surfactants, they could gradually

dissociate and release components by interacting with bio-amphiphilic molecules (such as the lipids of cell membranes) when retained with cells.

Besides Herceptin, interferon α-2a was loaded into MNCs (IFN–MNC) to illustrate the *in vitro* anticancer effect of the green tea-based carrier loaded with another therapeutic protein. IFN is used in combination with chemotherapy and radiation as a cancer treatment. It has been reported to inhibit the proliferation and induce the apoptosis of cancer cells in hepatocellular carcinoma[30]. IFN–MNC also showed a higher cancer cell growth inhibitory effect than free IFN on HAK-1B (human liver cancer cell line) due to synergism of the inhibitory effects of the carrier and IFN (CI = 0.46, Supplementary Fig. 11a).

In Fig. 4b, the anticancer effect of Herceptin–MNC was investigated and compared to that of free Herceptin, BSA–MNC (that is, drug-free carrier) and sequentially injected BSA–MNC and Herceptin using a BT-474-xenografted nude mouse model (Athymic Nude-Foxn1nu, female). The tumour treated with phosphate-buffered saline (PBS; vehicle control) progressed rapidly over 35 days. In contrast, Herceptin–MNC efficiently retarded tumour growth. Herceptin–MNC showed a significantly higher anticancer effect than sequentially injected BSA–MNC and Herceptin, as well as free Herceptin. During the period of treatment there was no significant difference in body weight and survival rate between groups (Supplementary Fig. 12). The mice showed no signs of toxicity (tachypnoea/dyspnoea, lethargy, diarrhoea and abnormal activity) or pathological changes to the organs (Supplementary Table 1). The results demonstrated the significant benefit of utilizing Herceptin–MNC in the BT-474 model, which could be attributed to the effects of combining Herceptin and the green tea-based MNCs.

IFN–MNC also showed a greatly enhanced anticancer effect on HAK-1B-xenografted nude mouse model (CrTac:NCr-Foxn1nu, female) when compared to free IFN, BSA–MNC (that is, drug-free carrier) and sequentially injected BSA–MNC and IFN (Supplementary Fig. 11b), with no significant difference in body weight and survival rate between groups (Supplementary Fig. 13).

To assess the effectiveness of Herceptin delivery, the biodistributions of Herceptin–MNC and free Herceptin in normal organs and a tumour were examined (Fig. 4c,d). Heptamethine near-infrared (NIR) fluorophore ZW800-1[31] was conjugated to Herceptin for this study (Supplementary Fig. 14). Herceptin–MNC exhibited a 2.3-fold higher accumulation in the tumour (8.4% injected dose/g organ, % ID/g) and 0.3-fold (2.1% ID/g), 0.3-fold (1.7% ID/g) and 0.6-fold (1.4% ID/g) lower accumulation in liver, kidney and lung, respectively, when compared to free Herceptin (3.7, 6.8, 6.0 and 2.4% ID/g, respectively) at 24 h post-injection. Herceptin–MNC showed over 29-fold longer blood half-life and significantly better tumour selectivity than free Herceptin (Fig. 4e, Supplementary Fig. 15). Similarly, when compared with free IFN, IFN–MNC exhibited 3.2-fold higher accumulation in the tumour (Supplementary Fig. 11c,d), and higher selectivity and longer blood half-life (Supplementary Figs 17 and 18). These results demonstrate that the protein–MNC is capable of delivering a substantially higher quantity of proteins into a tumour with high selectivity and with a prolonged period of blood circulation when compared to free proteins. The intratumoral microdistribution of Herceptin–MNC was examined to study extravasation and penetration of Herceptin–MNC in tumours (Fig. 4f). Herceptin–MNCs were distributed throughout the extravascular space at 24 h post-injection, which was consistent with the localization of HER2/neu receptors overexpressed on the tumour, suggesting extravasation and deep tumour penetration of Herceptin–MNC.

We have developed and characterized a green tea-based MNC for protein delivery where the carrier itself displays anticancer effects. This system was formulated by the simple self-assembly of EGCG derivatives and proteins, and showed restraint and restoration of protein activity upon complexation and dissociation, respectively. It effectively protected the proteins against many obstacles from the point of administration to the delivery sites. The combined therapeutic effects of the green tea-based carrier and the protein drug showed greater anticancer effect than the free protein.

Methods

Materials characterization. The size and polydispersity of the samples were evaluated by dynamic light scattering with a particle sizer (Brookhaven Instruments). The size and morphology of the samples were characterized with a TEM (FEI Tecnai G^2 F20 S-Twin, 200 kV).

Activity of xanthine oxidase, α-amylase and lysozyme. Xanthine oxidase activity was measured by determining uric acid production at 295 nm with a UV–vis spectrophotometer (Hitachi). α-Amylase activity was assayed with an activity kit (Molecular Probes, E-11954) using a fluorescence spectrophotometer (Hitachi, λ_{ex} = 505 nm and λ_{em} = 512 nm). Lysozyme activity was determined spectrophotometrically at 450 nm from the decrease in turbidity due to the cleavage of glucosidic linkages of *Micrococcus lysodeikticus*.

Cell culture. BT-474 cells (HTB-30) were purchased from ATCC, and were cultured in RPMI 1640 with HEPES buffer supplemented with 10% fetal bovine serum (FBS) and 100 units ml^{-1} of penicillin and streptomycin. The medium and supplements were purchased from Gibco.

Inhibitory effect in cancer cell proliferation. BT-474 cells were seeded (1×10^4 cells in RPMI 1640/well) in quintuplicate in 96-well microplates, and allowed to adhere overnight. The culture media were then replaced by media containing the following samples: Herceptin (0.5 mg ml^{-1}), Herceptin–MNC (Herceptin/OEGCG/PEG–EGCG = 0.5/0.024/0.26 mg ml^{-1}), BSA–MNC (BSA/OEGCG/PEG–EGCG = 0.5/0.024/0.26 mg ml^{-1}), a mixture of BSA–MNC and Herceptin (BSA/OEGCG/PEG–EGCG = 0.5/0.024/0.26 mg ml^{-1}; Herceptin = 0.5 mg ml^{-1}), BSA (0.5 mg ml^{-1}), OEGCG (0.024 mg ml^{-1}) and PEG–EGCG (0.26 mg ml^{-1}). The cells were incubated at 37 °C in 5% CO_2. After 72 h, the culture media were replaced by phenol red-free medium containing 10% Alamar Blue, which is a dye reduced by the cytochrome *c* activity of cells. Cell proliferation was determined from dye reduction by monitoring the fluorescence intensity (λ_{ex} = 549 nm and λ_{em} = 587 nm) after 4 h of incubation. The synergism of the inhibitory effects of the carrier and protein was quantified by the Chou-Talalay method using CalcuSyn software[32]. Statistical analysis was conducted using analysis of variance (ANOVA).

Anticancer effect in tumour-xenografted nude mice. Athymic Nude-Foxn1nu female mice were inoculated s.c. with 1×10^7 BT-474 cells suspended in 100 μl of PBS and 100 μl of Matrigel (BD Bioscience) in the right flank. One day before inoculation, 17 β-oestradiol pellets (0.72 mg, 60-day release, Innovative Research of America) were implanted s.c. in each mouse using a trocar. Once the tumours reached a volume of 270 mm^3, 12 mice per group were randomly allocated for different treatments. Treatment was administered twice weekly via i.v. injection for 35 days with PBS (vehicle control), free Herceptin, BSA–MNC, sequential administration of BSA–MNC and Herceptin, and Herceptin–MNC, in the same formulations as those used in the *in vitro* experiments. Tumours were measured twice weekly with a digital caliper, and the tumour volumes (mm^3) were calculated from the following formula: volume = (length × $width^2$)/2 (ref. 33). The care and use of laboratory animals were regulated according to protocols approved by the Institutional Animal Care and Use Committee (IACUC) at the Biological Resource Centre (BRC) in Biopolis, Singapore. Statistical analysis was conducted using ANOVA.

Real-time intraoperative imaging. Each compound (2–10 nmol) was injected intravenously into BT-474-xenografted athymic Nude-Foxn1nu mice. Animals were imaged at 24 h post-injection of Herceptin–MNC and free Herceptin using the fluorescence-assisted resection and exploration (FLARE) real-time intraoperative imaging system. Excitation fluorescence rates for white light and 800 nm NIR excitation light were 20,000 lux and 10 mW cm^{-2}, respectively. The fluorescence (FL) and background (BG) intensities of a region of interest (ROI) for each organ/tissue were quantified using custom FLARE software. The contrast-to-background ratio (CBR) was calculated as CBR = (FL – BG)/BG. At least five animals were analysed. Statistical analysis was conducting using a one-way ANOVA, followed by Tukey's multiple comparisons test.

Immunohistochemistry and NIR fluorescence microscopy. The polyclonal rabbit anti-human HER2 primary antibody (Dako) was used for the tumour tissue biopsies, diluted 1:50 from stock solution (10 μg ml^{-1}) and incubated at 4 °C overnight. Goat anti-rabbit secondary antibody labelled with Alexa Fluor 680 (Invitrogen) was incubated for 1 h at room temperature at a protein concentration of 250 nM. Antibody conjugates were fixed in place with 2% paraformaldehyde. The slides were mounted with Fluoromount-G and covered with a coverslip for microscopy. Serial sections were stained with haematoxylin and eosin (H&E) using an autostainer (Leica). NIR fluorescence microscopy was performed on a Nikon

TE300 with a four-channel Nikon TE300. The excitation and emission filters used were 650/45 nm and 710/50 nm for Alexa 680 imaging, and 750/50 nm and 810/40 nm for NIR targeted tumour imaging, respectively.

Received 26 November 2012; accepted 21 August 2014; published online 5 October 2014

References

1. Allen, T. M. & Cullis, P. R. Drug delivery systems: entering the mainstream. *Science* **303,** 1818–1822 (2004).
2. Cao, Y. & Cao, R. Angiogenesis inhibited by drinking tea. *Nature* **398,** 381 (1999).
3. Jankun, J., Selman, S. H., Swiercz, R. & Skrzypczak-Jankun, E. Why drinking green tea could prevent cancer. *Nature* **387,** 561 (1997).
4. Tachibana, H., Koga, K., Fujimura, Y. & Yamada, K. A receptor for green tea polyphenol EGCG. *Nature Struct. Mol. Biol.* **11,** 380–381 (2004).
5. Liang, G. *et al.* Green tea catechins augment the antitumor activity of doxorubicin in an *in vivo* mouse model for chemoresistant liver cancer. *Int. J. Oncol.* **37,** 111–123 (2010).
6. Garbisa, S. *et al.* Tumor invasion: molecular shears blunted by green tea. *Nature Med.* **5,** 1216 (1999).
7. Du, G. J. *et al.* Epigallocatechin gallate (EGCG) is the most effective cancer chemopreventive polyphenol in green tea. *Nutrients* **4,** 1679–1691 (2012).
8. Li, S., Hattori, T. & Kodama, E. N. Epigallocatechin gallate inhibits the HIV reverse transcription step. *Antivir. Chem. Chemother.* **21,** 239–243 (2011).
9. Yu, J. *et al.* Epigallocatechin-3-gallate protects motor neurons and regulates glutamate level. *FEBS Lett.* **584,** 2921–2925 (2010).
10. Morley, N. *et al.* The green tea polyphenol (–)-epigallocatechin gallate and green tea can protect human cellular DNA from ultraviolet and visible radiation-induced damage. *Photodermatol. Photoimmunol. Photomed.* **21,** 15–22 (2005).
11. Miyata, K., Christie, R. J. & Kataoka, K. Polymeric micelles for nano-scale drug delivery. *React. Funct. Polym.* **71,** 227–234 (2011).
12. Musacchio, T. & Torchilin, V. P. Recent developments in lipid-based pharmaceutical nanocarriers. *Front. Biosci.* **16,** 1388–1412 (2011).
13. Duncan, R. The dawning era of polymer therapeutics. *Nature Rev. Drug Discov.* **2,** 347–360 (2003).
14. Hubbell, J. A. Materials science. Enhancing drug function. *Science* **300,** 595–596 (2003).
15. Kopecek, J. & Kopeckova, P. HPMA copolymers: origins, early developments, present, and future. *Adv. Drug Deliv. Rev.* **62,** 122–149 (2010).
16. Duncan, R. Polymer conjugates as anticancer nanomedicines. *Nature Rev. Cancer* **6,** 688–701 (2006).
17. Farokhzad, O. C. *et al.* Nanoparticle–aptamer bioconjugates: a new approach for targeting prostate cancer cells. *Cancer Res.* **64,** 7668–7672 (2004).
18. Miura, Y. *et al.* Cyclic RGD-linked polymeric micelles for targeted delivery of platinum anticancer drugs to glioblastoma through the blood–brain tumor barrier. *ACS Nano* **7,** 8583–8592 (2013).
19. Cabral, H. *et al.* Targeted therapy of spontaneous murine pancreatic tumors by polymeric micelles prolongs survival and prevents peritoneal metastasis. *Proc. Natl Acad. Sci. USA* **110,** 11397–11402 (2013).
20. Wang, F. *et al.* Selective tissue distribution and long circulation endowed by paclitaxel loaded PEGylated poly(epsilon-caprolactone-co-L-lactide) micelles leading to improved anti-tumor effects and low systematic toxicity. *Int. J. Pharm.* **456,** 101–112 (2013).
21. Harris, J. M. & Chess, R. B. Effect of pegylation on pharmaceuticals. *Nature Rev. Drug Discov.* **2,** 214–221 (2003).
22. Kim, D., Gao, Z. G., Lee, E. S. & Bae, Y. H. *In vivo* evaluation of doxorubicin-loaded polymeric micelles targeting folate receptors and early endosomal pH in drug-resistant ovarian cancer. *Mol. Pharmacol.* **6,** 1353–1362 (2009).
23. Ishii, T. *et al.* Treatment of cerebral ischemia-reperfusion injury with PEGylated liposomes encapsulating FK506. *FASEB J.* **27,** 1362–1370 (2013).
24. Yang, C. S. & Wang, Z. Y. Tea and cancer. *J. Natl Cancer Inst.* **85,** 1038–1049 (1993).
25. Kuzuhara, T., Sei, Y., Yamaguchi, K., Suganuma, M. & Fujiki, H. DNA and RNA as new binding targets of green tea catechins. *J. Biol. Chem.* **281,** 17446–17456 (2006).
26. Chung, J. E., Kurisawa, M., Kim, Y. J., Uyama, H. & Kobayashi, S. Amplification of antioxidant activity of catechin by polycondensation with acetaldehyde. *Biomacromolecules* **5,** 113–118 (2004).
27. Saucier, C., Guerra, C., Pianet, I., Laguerre, M. & Glories, Y. (+)-Catechin-acetaldehyde condensation products in relation to wine-ageing. *Phytochemistry* **46,** 229–234 (1997).
28. Jobstl, E., O'Connell, J., Fairclough, J. P. & Williamson, M. P. Molecular model for astringency produced by polyphenol/protein interactions. *Biomacromolecules* **5,** 942–949 (2004).
29. Villalba, J. J. & Provenza, F. D. Preference for polyethylene glycol by sheep fed a quebracho tannin diet. *J. Anim. Sci.* **79,** 2066–2074 (2001).
30. Hisaka, T. *et al.* Interferon-αCon1 suppresses proliferation of liver cancer cell lines *in vitro* and *in vivo*. *J. Hepatol.* **41,** 782–789 (2004).
31. Choi, H. S. *et al.* Synthesis and *in vivo* fate of zwitterionic near-infrared fluorophores. *Angew. Chem. Int. Ed.* **50,** 6258–6263 (2011).
32. Chou, T. C., Motzer, R. J., Tong, Y. & Bosl, G. J. Computerized quantitation of synergism and antagonism of taxol, topotecan, and cisplatin against human teratocarcinoma cell growth: a rational approach to clinical protocol design. *J. Natl Cancer Inst.* **86,** 1517–1524 (1994).
33. Sun, J. *et al.* Antitumor efficacy of a novel class of non-thiol-containing peptidomimetic inhibitors of farnesyltransferase and geranylgeranyltransferase I: combination therapy with the cytotoxic agents cisplatin, taxol, and gemcitabine. *Cancer Res.* **59,** 4919–4926 (1999).

Acknowledgements

This research was funded by the Institute of Bioengineering and Nanotechnology (Biomedical Research Council, Agency for Science, Technology and Research, Singapore) and the National Institutes of Health (NIBIB grant no. R01-EB-011523, to H.S.C.). The authors thank A. Yamashita and J.P.K. Tan for their assistance with cell culture and TEM experiments, respectively.

Author contributions

J.E.C. and M.K. conceived and designed the experiments. J.E.C., S.T., N.Y. and S.J.G. performed the experiments. S.H.K., J.H.L. and H.S.C. performed experiments and analysed data regarding biodistribution and pharmacokinetics. H.Y. provided HAK-1B cells. J.E.C. and M.K. reviewed, analysed and interpreted the data. J.E.C., S.T., H.S.C., M.K and J.Y.Y wrote the paper. All authors discussed the results. J.E.C. and M.K. supervised the project.

Additional information

Supplementary information is available in the online version of the paper. Reprints and permissions information is available online at www.nature.com/reprints. Correspondence and requests for materials should be addressed to J.E.C. and M.K.

Competing financial interests

The authors declare no competing financial interests.

J Hepatobiliary Pancreat Sci (2014) ••:••–••
DOI: 10.1002/jhbp.177

ORIGINAL ARTICLE

Therapeutic efficacy of splenectomy is attenuated by necroinflammation of the liver in patients with liver cirrhosis

Reiichiro Kondo · Masayoshi Kage · Toshiro Ogata · Osamu Nakashima · Jun Akiba · Yoriko Nomura · Hirohisa Yano

Abstract
Background Splenectomy is a therapy for thrombocytopenia caused by hypersplenism with liver cirrhosis. However, the determinant of therapeutic outcomes for this complication has not yet been fully clarified.
Methods We studied the laboratory findings of 55 patients who underwent splenectomy for hypersplenism with liver cirrhosis. In addition, we examined the histopathological findings of hepatosplenic tissues of nine patients who underwent hepatectomy for hepatocellular carcinoma and splenectomy for hypersplenism with liver cirrhosis on one stage surgery. The locations of platelets in hepatosplenic tissues were identified by immunohistochemistry. We used monoclonal antibody against CD41.
Results Among 55 patients, 40 patients had high serum alanine aminotransferase (ALT) level (≧38 IU/l). Blood platelet count after splenectomy of patients with high serum ALT level were significantly lower than those of patients with low serum ALT level ($P = 0.02$). Histopathologically, platelet area of the liver tissues was positively correlated with hepatic inflammation ($P = 0.02$). Platelet area of the liver tissues was negatively correlated with blood platelet count after splenectomy ($P = 0.03$).
Conclusions Hepatic inflammation contributes to the accumulation of platelets in liver; therefore, in patients with high serum ALT level, improvement of thrombocytopenia by the elimination of hypersplenism was limited.

Keywords Alanine aminotransferase · Hepatitis C · Hypersplenism · Immunohistochemical analysis · Platelet

R. Kondo (✉) · J. Akiba · Y. Nomura · H. Yano
Department of Pathology, Kurume University School of Medicine, 67 Asahi-machi, Kurume, Fukuoka 830-0011, Japan
e-mail: kondou_reiichirou@kurume-u.ac.jp

R. Kondo · M. Kage
Cancer Center, Kurume University Hospital, Kurume, Fukuoka, Japan

R. Kondo · M. Kage · Y. Nomura
Department of Diagnostic Pathology, Kurume University Hospital, Kurume, Fukuoka, Japan

T. Ogata
Department of Surgery, Kurume University School of Medicine, Kurume, Fukuoka, Japan

O. Nakashima
Department of Clinical Laboratory Medicine, Kurume University Hospital, Kurume, Fukuoka, Japan

Introduction

Cirrhosis is a major cause of morbidity and mortality in many countries, and it results in liver failure, portal hypertension, and increased risk of carcinogenesis. In chronic hepatitis, the blood platelet decreased gradually to be reflected in the liver fibrosis. Thrombocytopenia is a marked feature of liver cirrhosis. Thrombocytopenia is of great relevance in the management of liver cirrhosis because of the widespread use of myelodepressant drugs such as interferon or antineoplastic agents. However, there is no standard therapy for this complication.

The role of platelets in the pathogenesis of liver damage and exact mechanisms leading to thrombocytopenia in liver cirrhosis has not yet been fully clarified. The platelet kinetics of patients with chronic liver disease are not well characterized. The mechanisms leading to thrombocytopenia with liver cirrhosis are most likely multifactorial processes combining increased splenic platelet breakdown [1–3], splenic pooling [4, 5], and the inability of the bone marrow to increase platelet production adequately [6].

In a recent study, we reported that the accumulation of platelets in the liver may be an important contributory factor

to thrombocytopenia in chronic hepatitis C [7]. Platelets in non-cancerous liver tissues of patients with chronic hepatitis or cirrhosis were seen predominantly in the sinusoidal space of the periportal area with inflammation. As viewed through an electron microscope, the platelets were aggregated in the sinusoids and adhered to the sinusoidal endothelial cells. Platelets may accumulate in the sinusoidal space under thombocytotic conditions in chronic hepatitis C brought about by the activated hepatic reticuloendothelial system caused by inflammation [7].

Splenectomy [8, 9] and partial splenic arterial embolization [10] are therapies for thrombocytopenia caused by hypersplenism with liver cirrhosis. The elimination of hypersplenism by splenectomy or partial splenic arterial embolization improves thrombocytopenia. The spleen and chronic liver disease are closely related. In this study, we evaluated the efficacy and determinant of therapeutic outcomes of splenectomy in the treatment of thrombocytopenia caused by hypersplenism with liver cirrhosis and investigated the interaction among the liver, spleen, and blood platelets in patients with liver cirrhosis.

Methods

Materials

We studied the laboratory findings of 55 patients who underwent splenectomy for thrombocytopenia caused by hypersplenism with hepatitis C viral infection associated liver cirrhosis at Kurume University Hospital between January 2005 and December 2012. There were 30 men and 25 women. The mean age was 60 ± 8 years (range, 42 to 77 years). In addition, we examined the histopathological findings of hepatosplenic tissues of nine patients with hepatitis C viral infection associated liver cirrhosis who underwent hepatectomy for hepatocellular carcinoma and splenectomy for hypersplenism on one stage surgery at Kurume University Hospital between January 1999 and December 2007. There were three men and six women. The mean age of patients was 59 ± 9 years (range, 41 to 70 years). Five specimens of liver tissue and nine specimens of splenic tissue without chronic hepatitis or thrombocytopenia that were obtained during surgery were used as normal control tissues.

Splenectomy was generally performed in hypersplenic patients with thrombocytopenia (platelet count $< 6 \times 10^4$/mm^3) or leukopenia (white blood cell count <3000 /μl). All patients did not receive myelodepressant drugs or preoperative anticancer therapies and there were no postoperative complications such as severe infection.

This study was performed with informed consent obtained from patients for the use of their laboratory data, liver tissues and splenic tissues in the investigation and was approved by the Ethical Committee at Kurume University, the approved ID number: 11 200.

Laboratory study

Blood samples of all patients were collected from a peripheral vein of the extremities before surgery and 3 months after. We estimated blood cell count, serum alanine aminotransferase (ALT) level, serum total bilirubin level, serum albumin level, and prothrombin time.

Histopathology

Non-cancerous liver tissues and splenic tissues from nine patients who underwent hepatectomy and splenectomy on one stage surgery were obtained during surgery. Each tissue, fixed with 10% formalin embedded in paraffin, and cut into 5-μm sections, was used for histological and immunohistochemical analyses. Specimens were stained with hematoxylin and eosin and examined under a light microscope.

The histologic liver damage of these specimens was evaluated for fibrosis and inflammation according to the classification proposed by the International Association for the Study of the Liver [11, 12]. The severity of fibrosis was classified as none: stage 0, portal fibrosis: stage 1, periportal fibrosis: stage 2, bridging fibrosis with lobar distortion: stage 3, and cirrhosis: stage 4. The inflammatory activity was classified as none: grade 0, minimal: grade 1, mild: grade 2, moderate: grade 3, or severe: grade 4. Histopathological diagnosis was performed by three pathologists (RK, ON and MK).

Immunohistochemical analysis

An immunohistochemical study was performed using the streptavidin-biotin method. We used monoclonal antibody against CD41 (1:500, Beckman Coulter, Brea, CA, USA). 3, 3'-diaminobenzidine (DAB) was used as the chromogen in the immunostaining. CD41 (α II b integrin) is a specific marker for platelets [13]. Among CD41-positive cells, those without nuclei were evaluated as platelets and those with large, irregular shaped nuclei were evaluated as megakaryocytes.

Measurement of cells

The platelet area was measured using a WinROOF software package (version 6.1, Mitani Corporation, Fukui, Japan). In liver tissues, the platelet area was measured in five

Table 1 Clinical features of 55 patients with splenectomy

	Before splenectomy	3 months after splenectomy	*P*-value
Blood white cell count (/μl)[a]	2,960 ± 1,236 (1,100–8,200)	4,965 ± 1,859 (2,400–11,100)	<0.01
Blood red cell count (/μl)[a]	393 ± 51 (306–520)	387 ± 49 (288–503)	0.56
Blood platelet count ($\times 10^4$/mm^3)[a]	4.4 ± 1.5 (1.4–7.7)	17.5 ± 7.6 (6.1–47.4)	<0.01
ALT (IU/l)[a]	55 ± 24 (18–157)	42 ± 16 (15–91)	<0.01
T. bil (mg/dl)[a]	1.4 ± 0.7 (0.5–4.8)	1.1 ± 0.5 (0.4–2.9)	<0.01
PT (%)[a]	72 ± 12 (49–94)	66 ± 15 (36–96)	0.04
Alb (g/dl)[a]	3.5 ± 0.4 (2.4–4.5)	3.5 ± 0.5 (2.3–4.6)	0.77

Alb serum albumin level, *ALT* serum alanine aminotransferase level, *PT* prothrombin percentage activity, *T.bil* serum total bilirubin level
[a]Mean ± SD (range)

Table 2 Comparison of preoperative patient characteristics based on therapeutic effect of splenectomy

	Limited response group (n = 30)	Response group (n = 25)	*P*-value
Gender (male / female)	16 / 14	9 / 16	0.2
Age (years)[a]	61 ± 8	60 ± 8	0.97
Blood white cell count (/μl)[a]	3,067 ± 1,396	2,832 ± 1,026	0.49
Blood red cell count (/μl)[a]	378 ± 40	412 ± 58	0.01
Blood platelet count ($\times 10^4$/mm^3)[a]	4.3 ± 1.6	4.5 ± 1.4	0.73
ALT (IU/l) (< 38 / ≧ 38)	5 / 25	10 / 15	0.05
T. bil (mg/dl)[a]	1.4 ± 0.9	1.3 ± 0.5	0.61
PT (%)[a]	75 ± 9	68 ± 13	0.04
Alb (g/dl)[a]	3.4 ± 0.4	3.6 ± 0.4	0.06

Alb serum albumin level, *ALT* serum alanine aminotransferase level, *PT* prothrombin percentage activity, *T.bil* serum total bilirubin level
[a]Mean ± SD (range)

periportal and five lobule areas randomly selected. In splenic tissues, five visual fields in the red pulp were randomly selected.

Statistical analysis

All data are expressed as the mean ±standard deviation (SD). Quartile value was determined for the measured variables. Comparisons between two groups of patients, those based on blood platelet count after splenectomy, were performed using the Mann–Whitney *U*-test for continuous variables, and χ^2 test for discrete variables. Only variables that demonstrated a *P*-value of under 0.05 in the univariate analysis were entered into a multiple logistic regression model to identify factors associated with blood platelet count after splenectomy. Pearson correlation coefficients were calculated to examine the association of blood platelet count after splenectomy and preoperative serum ALT level. *P*-values less than 0.05 were considered to indicate significance. Statistical analysis was performed using a JMP software package (Release 11.0, SAS Institute, Cary, NC, USA).

Results

Laboratory findings of 55 patients who underwent splenectomy

Summary of laboratory findings of 55 cirrhotic patients who underwent splenectomy are shown in Table 1. Blood platelet count, blood white cell count and serum total bilirubin level significantly improved 3 months after splenectomy. The mean value of blood platelet count 3 months after splenectomy was 17.5 × 10^4/mm^3. The mean value and quartile value of serum ALT level before splenectomy were 55 IU/l and 37 IU/l, respectively. The Response group, in which the blood platelet counts 3 months after splenectomy were over 17.5 × 10^4/mm^3, was 25 patients and the Limited response group, in which the blood platelet count 3 months after splenectomy was under 17.5 × 10^4/mm^3, was 30 patients. The preoperative characteristics of the two-patient response group are shown in Table 2. There was significant difference of blood red cell count, serum ALT level, and prothrombin time between the Response group and Limited response group.

Table 3 Predictor of blood platelet count after splenectomy by multiple logistic regression analysis in 55 patients with splenectomy

	OR (95% CI)	*P*-value
Blood red cell count before splenectomy (≧380 /μl)	2.41 (0.75–8.52)	0.14
ALT level before splenectomy (<38 IU/l)	3.4 (0.96–13.44)	0.05
PT level before splenectomy (<75%)	2.7 (0.83–9.53)	0.1

ALT serum alanine aminotransferase level; *CI* confidence interval, *OR* odds ratio, *PT* prothrombin percentage activity

Multiple logistic regression analysis was performed to identify which variables were independently associated with the blood platelet count 3 months after splenectomy (Table 3). Preoperative serum ALT level was independent predictors of the blood platelet count 3 months after splenectomy (<38 IU/l, OR 3.4, 95% CI 0.96–13.44, $P = 0.05$).

Blood platelet count and serum ALT level

Among 55 patients, 40 patients had high serum ALT level (≧38 IU/l). In both patients with high ALT level and low ALT level, blood platelet count significantly improved 3 months after splenectomy (low serum ALT patients, $n = 15$, from $4.2 \pm 1.3 \times 10^4/mm^3$ to $21.2 \pm 10 \times 10^4/mm^3$, $P < 0.01$; Fig. 1a) (high serum ALT patients, $n = 40$, from $4.5 \pm 1.6 \times 10^4/mm^3$ to $16 \pm 6 \times 10^4/mm^3$, $P < 0.01$; Fig. 1b). Three months after splenectomy, blood platelet count of patients with high serum ALT level were significantly lower than those of patients with low serum ALT level ($P = 0.02$) (Fig. 1c). In 55 cirrhotic patients who underwent splenectomy, blood platelet count 3 months after splenectomy decreased along with an increase in preoperative serum ALT level ($r = 0.67$, $P = 0.03$) (Fig. 1d).

Pathological findings of liver tissues

In nine patients who underwent hepatectomy and splenectomy on one stage surgery, all non-cancerous liver tissues showed bridging fibrosis with diffuse lobar distortion (stage 4) (Fig. 2a). In patients with liver cirrhosis, platelets were present predominantly in the sinusoids of the periportal area with inflammation. In cirrhotic patients with high serum ALT level, platelets were observed along the destructed limiting plate of the expanded fibrous portal area with inflammation and in the sinusoids of the periportal area (Fig. 2b,c). In all liver tissues including normal controls and nine cirrhotic patients who underwent hepatectomy and splenectomy on one stage surgery, there were platelets but no megakaryocytes in the sinusoids. Liver tissues of patients with high serum ALT level showed a significantly higher degree of inflammation than those of patients with low serum ALT level (grade; 2 ± 1 vs. 1 ± 1, $P = 0.03$) (Fig. 3a). In control liver tissues, there were a few lymphocytes, but only in the portal area, and neither necroinflammatory reactions nor fibrosis were noted (grade 0, stage 0).

Morphometry revealed that patients with cirrhosis had more extensive platelet area in the liver tissues than controls. In nine cirrhotic patients who underwent hepatectomy and splenectomy, the platelet area in liver tissues increased along with an increase in a grade of hepatic inflammation ($r = 0.86$, $P = 0.02$) (Fig. 3b). Blood platelet count 3 months after splenectomy was negatively correlated with platelet area of the liver tissues by Pearson correlation calculations ($r = 0.49$, $P = 0.03$) (Fig. 3c). There was no significant correlation between platelet area of the liver tissues and blood platelet count before splenectomy ($r = 0.01$, $P = 0.83$) (Fig. 3d). In patients with liver cirrhosis, the platelet area in liver tissues of patients with high serum ALT level were larger than those of patients with low serum ALT level ($18\,233 \pm 11\,188\ \mu m^2$ vs. $6672 \pm 5257\ \mu m^2$, $P = 0.14$).

Pathological findings of splenic tissues

In all splenic tissues, including cirrhotic patients with high or low serum ALT level and normal controls, platelets were diffusely found in the splenic sinus and splenic cord of the red pulp (Fig. 4a,b). Among the splenic tissues of nine cirrhotic patients who underwent hepatectomy and splenectomy on one stage surgery, megakaryocytes were observed in those of six patients (67%). CD41-positive-megakaryocytes were present in the splenic cord of the red pulp (Fig. 4c). There were no megakaryocytes in normal control tissues. Platelet area in splenic tissues of cirrhotic patients with high serum ALT level and those of patients with normal serum ALT level were $47\,685 \pm 22\,806\ \mu m^2$ and $78\,550 \pm 6550\ \mu m^2$, respectively.

Discussion

The exact mechanisms leading to thrombocytopenia in liver cirrhosis and the platelet kinetics of patients with chronic liver disease or cirrhosis are not well characterized. In this study, we demonstrated the histopathological findings of platelets in human hepatosplenic tissue and investigated the interaction between blood platelets and platelets of hepatosplenic tissues in cirrhotic patients.

Splenectomy [8, 9] and partial splenic arterial embolization [10] are therapies for thrombocytopenia caused by hypersplenism. Platelet kinetic studies using platelet scintigraphy have been reported [1, 2, 14–16].

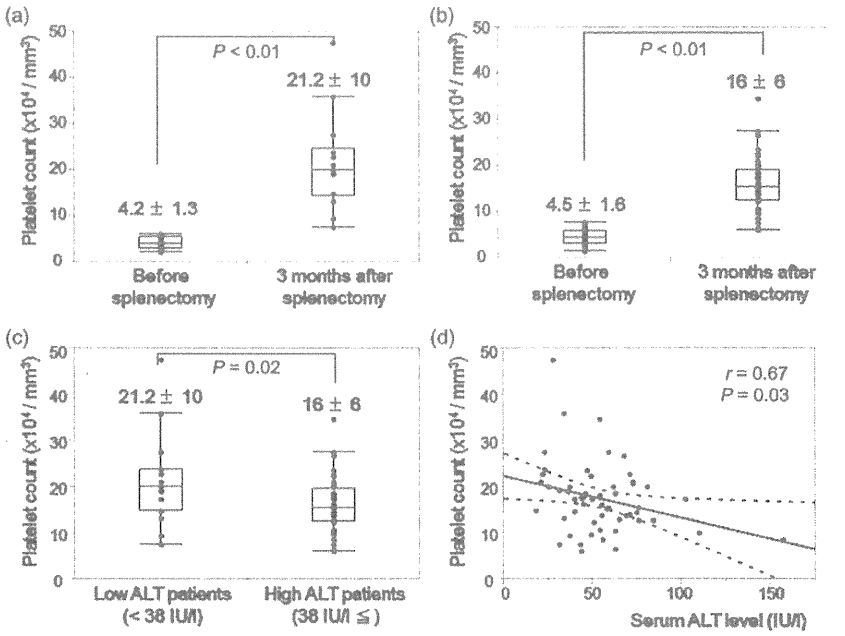

Fig. 1 Relationship between serum alanine aminotransferase (ALT) level and blood platelet count in 55 patients with splenectomy. (**a**) In 15 patients with low ALT level, comparison of the blood platelet count between before splenectomy and 3 months after. (**b**) In 40 patients with high ALT level, comparison of the blood platelet count between before splenectomy and 3 months after. (**c**) Three months after splenectomy, comparison of the blood platelet count between patients with high and low serum ALT level. (**d**) Correlation with the preoperative serum ALT level and the blood platelet count 3 months after splenectomy

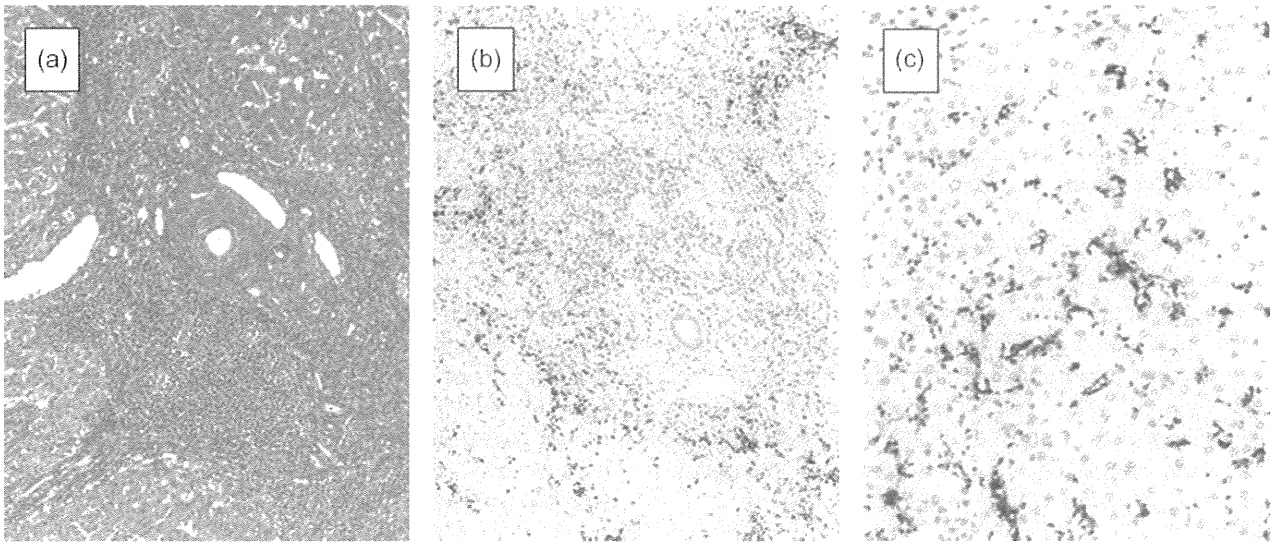

Fig. 2 Pathological findings of the liver tissues. (**a**) In liver tissue of cirrhotic patient with high serum alanine aminotransferase (ALT) level, there are strong inflammatory reactions in the portal area and destroyed limiting plate. Serum ALT 89 IU/l, grade 3, stage 4, stained with hematoxylin and eosin, × 100. (**b**) In liver tissue of cirrhotic patient with high serum ALT level, strong CD41 positive reactions are observed predominantly along the destroyed limiting plate of the expanded fibrous portal area with inflammation and in the sinusoidal space of the periportal area. Serum ALT 89 IU/l, grade 3, stage 4, immunostained with antibody against CD41, × 100. (**c**) Close up view of **b**. immunostained with antibody against CD41, × 200

Noguchi et al. [14] reported that partial splenic arterial embolization induced an increase in the blood platelet count and a decrease in the spleen/liver uptake ratio of ^{111}In-labeled platelets. In patients with thrombocytopenia, Kinuya et al. [15] reported that the spleen/liver uptake ratio for ^{111}In- or ^{99}Tc-labeled platelets was apparently lower in patients for whom splenectomy was ineffective than in those for whom it was effective. Based on these previous reports, splenectomy and partial splenic arterial embolization induce a decrease in platelet pooling or breakdown in the spleen of thrombocytopenic patients, and, as a result, the blood platelet count increased.

In this study, we found that blood platelet counts of cirrhotic patients with high serum ALT levels tended to only slightly improve after splenectomy. In a recent study, we reported that the accumulation of platelets in the liver with

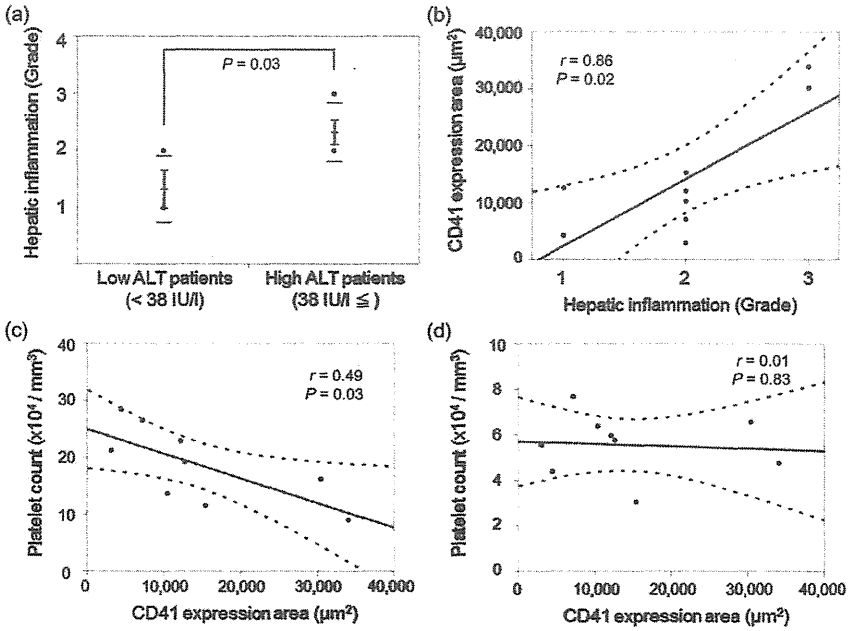

Fig. 3 Relationship between serum alanine aminotransferase (ALT) level, histologic inflammatory activity of liver tissues, and blood platelet count. (**a**) Comparison of the histologic inflammatory activity of liver tissues between patients with high and low serum ALT level. (**b**) Correlation with the platelet area of liver tissues and the histologic inflammatory activity of liver tissues. (**c**) Correlation with platelet area of liver tissues and the blood platelet count 3 months after splenectomy. (**d**) Correlation with platelet area of liver tissues and the blood platelet count before splenectomy

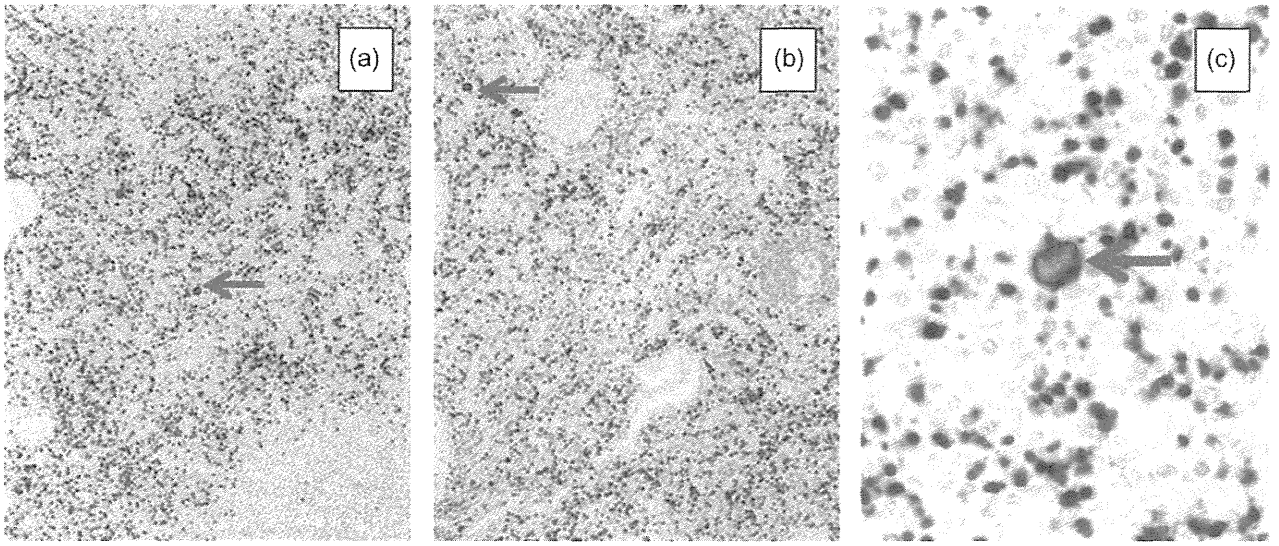

Fig. 4 Pathological findings of splenic tissues. (**a, b**) In the splenic tissue of cirrhotic patient with low (**a**) or high (**b**) serum alanine aminotransferase (ALT) level, CD41 positive reactions are diffusely observed in the splenic sinus and splenic cord of the red pulp. Megakaryocyte (arrow) is encountered in the splenic cord. immunostained with antibody against CD41, × 40; (**a**) Serum ALT 8 IU/l, grade 1, stage 4; (**b**) Serum ALT 89 IU/l, grade 3, stage 4. (**c**) Close up view of **b**. immunostained with antibody against CD41, × 200

chronic hepatitis and cirrhosis is one of the important contributory factors to thrombocytopenia [7]. The accumulation of platelets in noncancerous liver tissues of patients with chronic hepatitis or cirrhosis increased with an increase in the histological liver damage [7]. Platelets may accumulate in the sinusoids under thrombocytotic conditions in chronic hepatitis brought about by the activated hepatic reticuloendothelial system, as caused by inflammation [7, 17–20].

In blood vessels, the vessel wall, with its inner lining of endothelium, is crucial to the maintenance of a patent vasculature. The endothelium contains thromboregulators, nitric oxide, prostacyclin, and the ectonucleotidase CD39, which together provide a defense against platelet thrombus formation [21]. When the endothelium is disrupted, collagen and tissue factor become exposed to the flowing blood, thereby initiating the formation of thrombus. Endothelium

is also an important target for tumor necrosis factor (TNF) and interleukin-1 (IL-1). The endothelium synthesizes and releases platelet activating factor (PAF) in response to TNF. This activity of TNF overlaps that of IL-1, which also induces PAF production in endothelium [22]. These vessel wall alterations result in a change of endothelium from antithrombotic to thrombotic. The disrupted endothelium is the first reaction in platelet adhesion to the vessel subendothelium under physiologic blood flow [21]. In liver tissues injured by inflammation, platelets adhere to endothelial cells of sinusoids in the same way as to vessel walls [17]. A model of hepatitis, Kupffer cells produce the majority of TNF-α [23]. Under lipopolysaccharide administration in mice, TNF or IL-1 induces platelets to accumulate in the liver sinusoidal space within a few minutes by a different mechanism of aggregation [18–20].

In this study, the liver tissues of cirrhotic patients with high serum ALT level showed a significantly higher degree of inflammation than those of patients with low serum ALT level. We confirmed that, in patients with liver cirrhosis, the platelet area of the liver tissues was positively correlated with the degree of histological hepatic inflammation and negatively correlated with blood platelet count 3 months after splenectomy. In liver cirrhosis, chronic hepatic necroinflammation contributes to the accumulation of platelets in liver. We considered that patients with high serum ALT level had larger amount of platelets in liver than patients with low serum ALT level; as a result, they tended to only slightly improve thrombocytopenia after splenectomy. The mechanisms leading to thrombocytopenia with liver cirrhosis are most likely multifactorial processes [1–7]. The accumulation of platelets in the liver with chronic hepatitis and cirrhosis may be one of the important contributing factors to the therapeutic efficacy of splenectomy for thrombocytopenia.

In addition, we found megakaryocytes in the splenic tissues of most cirrhotic patients. This study also demonstrated that, in cirrhotic patients, blood platelet count and white blood cell count were higher after splenectomy than preoperative data. We considered that splenic megakaryocytes could not play major roles in platelet recovery in thrombocytopenia caused by hypersplenism with liver cirrhosis. Further biological studies should be undertaken to clarify the mechanisms and functions of megakaryopoiesis in the spleen.

In this study, in cirrhotic patients, serum total bilirubin level was lower after splenectomy compared with preoperative data. Bilirubinemia secondary to hypersplenism is caused by an increase in bilirubin production, which overloads the capacity of the liver to metabolize bilirubin [24]. To date, several reports have shown that a splenectomy accelerated hepatic regeneration and inhibits the formation of hepatic fibrosis [25–28]. Splenectomy may contribute to the decrease in total bilirubin level, but it is difficult to demonstrate any direct contribution, and care to protect liver function after operation could well have some influence.

In conclusion, in patients with liver cirrhosis, hepatic necroinflammation contributes to the accumulation of platelets in liver; therefore, in patients with high serum ALT level, improvement of thrombocytopenia by the elimination of hypersplenism was limited. Moreover, our results suggest that, in cirrhotic patients with thrombocytopenia caused by hypersplenism, serum ALT level may be a useful surrogate marker to predict the outcome of splenectomy. Additional large size and long-term studies should be undertaken to clarify this suggestion.

Acknowledgments This study was partially supported by a Health and Labor Sciences Research Grant from the Ministry of Health, Labor and Welfare Japan, regarding Research on Intractable Diseases, Portal Hemodynamic Abnormalities.

Conflict of interest None declared.

References

1. Aoki Y, Hirai K, Tanikawa K. Mechanism of thrombocytopenia in liver cirrhosis: kinetics of indium-111 tropolone labelled platelets. Eur J Nucl Med. 1993;20:123–9.
2. Schmidt KG, Rasmussen JW, Bekker C, Madsen PE. Kinetics and in vivo distribution of 111-in-labelled autologous platelets in chronic hepatic disease: mechanisms of thrombocytopenia. Scand J Haematol. 1985;34:39–46.
3. Pockros PJ, Duchini A, McMillan R, Nyberg LM, McHutchison J, Viernes E. Immune thrombocytopenic purpura in patients with chronic hepatitis C virus infection. Am J Gastroenterol. 2002;97:2040–5.
4. Aster RH. Pooling of platelets in the spleen: role in the pathogenesis of "hypersplenic" thrombocytopenia. J Clin Invest. 1966; 45:645–57.
5. Peck-Radosavljevic M. Thrombocytopenia in liver disease. Can J Gastroenterol. 2000;14(Suppl D):60D–6D.
6. Giannini E, Botta F, Borro P, Malfatti F, Fumagalli A, Testa E, et al. Relationship between thrombopoietin serum levels and liver function in patients with chronic liver disease related to hepatitis C virus infection. Am J Gastroenterol. 2003;98:2516–20.
7. Kondo R, Yano H, Nakashima O, Tanikawa K, Nomura Y, Kage M. Accumulation of platelets in the liver may be an important contributory factor to thrombocytopenia and liver fibrosis in chronic hepatitis C. J Gastroenterol. 2013;48:526–34.
8. Coon WW. Splenectomy for thrombocytopenia due to secondary hypersplenism. Arch Surg. 1988;123:369–71.
9. Kercher KW, Carbonell AM, Heniford BT, Matthews BD, Cunningham DM, Reindollar RW. Laparoscopic splenectomy reverses thrombocytopenia in patients with hepatitis C cirrhosis and portal hypertension. J Gastrointest Surg. 2004;8:120–6.
10. Sangro B, Bilbao I, Herrero I, Corella C, Longo J, Beloqui O, et al. Partial splenic embolization for the treatment of hypersplenism in cirrhosis. Hepatology. 1993;18:309–14.
11. Desmet VJ, Gerber M, Hoofnagle JH, Manns M, Scheuer PJ. Classification of chronic hepatitis: diagnosis, grading and staging. Hepatology. 1994;19:1513–20.

12. Batts KP, Ludwig J. Chronic hepatitis. An update on terminology and reporting. Am J Surg Pathol. 1995;19:1409–17.
13. Duperray A, Troesch A, Berthier R, Chagnon E, Frachet P, Uzan G, et al. Biosynthesis and assembly of platelet GPIIb-IIIa in human megakaryocytes: evidence that assembly between pro-GPIIb and GPIIIa is a prerequisite for expression of the complex on the cell surface. Blood. 1989;74:1603–11.
14. Noguchi H, Hirai K, Aoki Y, Sakata K, Tanikawa K. Changes in platelet kinetics after a partial splenic arterial embolization in cirrhotic patients with hypersplenism. Hepatology. 1995;22: 1682–8.
15. Kinuya K, Matano S, Nakashima H, Taki S. Scintigraphic prediction of therapeutic outcomes of splenectomy in patients with thrombocytopenia. Ann Nucl Med. 2003;17:161–4.
16. Sata M, Yano Y, Yoshiyama Y, Ide T, Kumashiro R, Suzuki H, et al. Mechanism of thrombocytopenia induced by interferon therapy for chronic hepatitis B. J Gastroenterol. 1997;32: 206–10.
17. Miyazawa Y, Tsutsui H, Mizuhara H, Fujiwara H, Kaneda K. Involvement of intrasinusoidal hemostasis in the development of concanavalin A-induced hepatic injury in mice. Hepatology. 1998;27:497–506.
18. Nakamura M, Shibazaki M, Nitta Y, Endo Y. Translocation of platelets into Disse spaces and their entry into hepatocytes in response to lipopolysaccharides, interleukin-1 and tumour necrosis factor: the role of Kupffer cells. J Hepatol. 1998;28:991–9.
19. Itoh H, Cicala C, Douglas GJ, Page CP. Platelet accumulation induced by bacterial endotoxin in rats. Thromb Res. 1996;83:405–19.
20. Pearson JM, Schultze AE, Jean PA, Roth RA. Platelet participation in liver injury from Gram-negative bacterial lipopolysaccharide in the rat. Shock. 1995;4:178–86.
21. Furie B, Furie BC. Mechanisms of thrombus formation. N Engl J Med. 2008;359:938–49.
22. Bussolino F, Camussi G, Baglioni C. Synthesis and release of platelet-activating factor by human vascular endothelial cells treated with tumor necrosis factor or Interleukin 1α. J Biol Chem. 1988;263:11856–61.
23. Dolganiuc A, Norkina O, Kodys K, Catalano D, Bakis G, Marshall C, et al. Viral and host factors induce macrophage activation and loss of toll-like receptor tolerance in chronic HCV infection. Gastroenterology. 2007;133:1627–36.
24. Sugawara Y, Yamamoto J, Shimada K, Yamasaki S, Kosuge T, Takayama T, et al. Splenectomy in patients with hepatocellular carcinoma and hypersplenism. J Am Coll Surg. 2000;190: 446–50.
25. Akahoshi T, Hashizume M, Tanoue K, Shimabukuro R, Gotoh N, Tomikawa M, et al. Role of the spleen in liver fibrosis in rats may be mediated by transforming growth factor β-1. J Gastroenterol Hepatol. 2002;17:59–65.
26. Ueda S, Yamanoi A, Hishikawa Y, Dhar DK, Tachibana M, Nagasue N. Transforming growth factor β-1 released from the spleen exerts a growth inhibitory effect on liver regeneration in rats. Lab Invest. 2003;83:1595–603.
27. Morinaga A, Ogata T, Kage M, Kinoshita H, Aoyagi S. Comparison of liver regeneration after a splenectomy and splenic artery ligation in a dimethylnitrosamine-induced cirrhotic rat model. HPB. 2010;12:22–30.
28. Nomura Y, Kage M, Ogata T, Kondou R, Kinoshita H, Ohshima K, et al. Influence of splenectomy in patients with liver cirrhosis and hypersplenism. Hepatol Res. 2014;44: E100–9.

消化器内科，59(2)：194-200，2014

特集II 門脈圧亢進症の治療法の選択とその成績

肝臓への血小板集積は肝硬変における脾摘の効果に関与するか*

近藤礼一郎**,***,****
矢野博久**
鹿毛政義***,****

Key Words：thrombocytopenia, platelet, transforming growth factor-beta(TGF-β), megakaryocyte

はじめに

末梢血血小板数減少は，慢性肝炎・肝硬変の重要な合併症である．慢性肝炎・肝硬変に伴う末梢血血小板減少の発生機序としては，脾臓への血小板のpooling[1]や脾臓での血球破壊の亢進[2]，骨髄での産生低下[3]など複数の病態が報告されている．最近，われわれは，慢性肝炎・肝硬変において，肝臓内にみられる血小板は肝線維化に伴い漸増し，肝臓への血小板集積も慢性肝炎・肝硬変に伴う末梢血血小板減少の重要な病態であることを報告した[4]．慢性肝炎・肝硬変に伴う末梢血血小板減少の治療として，脾機能亢進症を有する症例には脾臓摘出手術(脾摘)[5]や部分的脾動脈塞栓術(PSE)[6]が用いられているが，その治療成績と肝臓への血小板集積の関係は検討されていない．

また，近年，脾摘やPSEは，末梢血血小板減少の改善だけでなく，肝機能や肝線維化の改善にも寄与することが報告されている[7)~10)]．最近のわれわれの検討では，脾機能亢進症を有する肝硬変症例7例に対して脾摘時と脾摘後に肝生検を行い，4例で脾摘後に肝線維化の改善が病理組織学的に確認された[10]．慢性肝炎・肝硬変の病態における脾機能亢進症は，末梢血血小板減少だけに止まらず，重要な意味を持つことが示唆されている．

脾機能亢進症と肝線維化については，脾臓でのtransforming growth factor-β1(TGF-β1)の産生が関与していると報告されている[7)~9)]．肝硬変での脾機能亢進症では，脾臓でのTGF-β1産生が増加し，産生されたTGF-β1は門脈血を介して肝線維化に寄与しているとされている[7]．脾臓でのTGF-β1産生にはマクロファージの関与が報告されているが，十分には明らかにされていない[7)8)]．

本研究では，肝臓への血小板集積が，肝硬変による末梢血血小板減少に対する脾摘の効果に関与するかを検討した．さらに，脾臓におけるTGF-β1発現について病理学的な検討を行った．

方　法

肝細胞癌のため一期的に肝切除と脾摘を行った脾機能亢進症合併肝硬変症例12例(C型肝炎：9例，B型肝炎：1例，自己免疫性肝炎：1例，非アルコール性脂肪性肝炎：1例，平均年齢：61±9歳)を対象として用いた．なお，コントロールとして慢性肝炎，脾腫，末梢血血小板減少を伴わない外

* Accumulation of platelets in the liver may be an important contributing factor to the therapeutic efficacy of splenectomy in patients with liver cirrhosis.

** Reiichiro KONDO, M.D., Ph.D. & Hirohisa YANO, M.D., Ph.D.: 久留米大学医学部病理学講座〔〒830-0011 福岡県久留米市旭町67〕; Department of Pathology, Kurume University School of Medicine, Kurume, Fukuoka 830-0011, JAPAN
*** Masayoshi KAGE, M.D., Ph.D.: 久留米大学病院病理部
**** 久留米大学病院腫瘍センター

表1 血液検査所見まとめ

	ALT<38 IU/l(n=5)	ALT≧38 IU/l(n=7)
末梢血白血球数(/μl)		
脾摘前	2,960±829(2,100～4,300)	2,886±570(2,100～4,000)
脾摘3か月後	5,520±3,014(3,300～10,400)	5,028±1,490(2,400～6,700)
末梢血赤血球数(/μl)		
脾摘前	365±56(273～417)	403±45(343～476)
脾摘3か月後	333±56(255～377)	384±60(324～503)
末梢血血小板数($\times10^4/mm^3$)		
脾摘前	5.6±1.5(4.4～8)	6±1.6(3.1～7.7)
脾摘3か月後	26±7.5(17.4～35.8)	19.4±7.9(9.2～29.7)
ALT(IU/l)		
脾摘前	13±7(6～24)	59±19(38～89)
脾摘3か月後	18±10(8～32)	48±17(25～72)
T. bil(mg/dl)		
脾摘前	1.1±0.5(0.5～1.7)	1.1±0.3(0.7～1.5)
脾摘3か月後	0.7±0.2(0.4～0.9)	0.9±0.5(0.5～1.9)
PT(%)		
脾摘前	76±8(68～89)	82±11(69～99)
脾摘3か月後	81±15(65～100)	74±10(61～89)
Alb(g/dl)		
脾摘前	3.6±0.2(3.3～3.8)	3.8±0.5(3.1～4.5)
脾摘3か月後	3.6±0.4(3～4)	3.7±0.5(3.2～4.6)

科切除症例(肝臓5例，脾臓9例)を用いた．

1．臨床的検討

対象において，脾摘前と脾摘3か月後の血液検査所見を検討した．

2．病理組織学的検討

全症例の肝組織に対して，ヘマトキシリン・エオジン(HE)染色を行い，新犬山分類を用いて肝線維化と炎症の評価を行った．

次に，すべての肝組織と脾組織にCD41(αIIb integrin)とTGF-β1の免疫組織化学を行い，組織内の血小板，巨核球とTGF-β1発現を病理学的に検討した．CD41は血小板，巨核球に対する特異的な表面マーカーである[11]．

また，鏡検下で肝組織から門脈域周囲5か所，脾組織から赤脾髄5か所を無作為に選択し，血小板面積とTGF-β1陽性面積を画像解析ソフト(Win ROOF software package version 6.1, Mitani Corporation, Fukui, Japan)を用いて測定した．

結　果

1．臨床的検討

対象の血液検査所見のまとめを表1に示す．術前の血中ALT値が基準値である38 IU/l未満であった症例(ALT基準値内症例)は5例で，術前の血中ALT値が38 IU/l以上であった症例(高ALT症例)は7例であった．ALT基準値内症例，高ALT症例のいずれにおいても脾摘後に末梢血血小板数が改善したが，ALT基準値内症例と高ALT症例を比較すると，高ALT症例はALT基準値内症例より脾摘3か月後の末梢血血小板数改善が乏しかった(図1)(末梢血血小板数，脾摘前 → 脾摘3か月後，$6\pm1.6\times10^4/mm^3 \rightarrow 19.4\pm7.9\times10^4/mm^3$ vs. $5.6\pm1.5\times10^4/mm^3 \rightarrow 26\pm7.5\times10^4/mm^3$，$P=0.14$)．

2．病理組織学的検討

(1)肝臓の線維化と炎症

対象の全症例で，肝組織にはびまん性に，小葉のひずみを伴う線維性架橋形成がみられた(新犬山分類F4)．肝組織にみられる炎症は，高ALT症例の多くに門脈域の限界板を破壊した炎症がみられ，高ALT症例にみられる炎症はALT基準値内症例より有意に高度であった(図2)(新犬山分類A，2±1 vs. 1±1，$P=0.01$)．

コントロールの肝組織には，肝線維化や壊死炎症反応はみられなかった(新犬山分類F0 A0)．

(2)肝組織内の血小板と巨核球

コントロールを含む全症例で肝組織の類洞に血小板が観察された．コントロールでは，肝小葉の類洞に散在性に血小板がみられたが，対象では炎症が強い門脈域周囲の類洞に血小板が集積していた．高ALT症例では，炎症によって破壊された門脈域の限界板に沿って，またはその周囲の類洞に血小板の集積がみられた(図3)．肝組織内の血小板面積は，高ALT症例がALT基準値内症例より大きかった(図3)(15,217±8,058 μm² vs. 8,745±5,970 μm²，P=0.16)．対象とコントロールを含めて，肝組織内に巨核球はまったく認めなかった．

(3)脾組織内の血小板と巨核球

コントロールを含む全症例の脾組織で，血小板は赤脾髄の脾洞および脾索に，びまん性にみられた．また，対象12例のうち，9例(75%)で赤脾髄の脾索に巨核球を認めた．コントロールの脾組織に巨核球は認めなかった．脾組織内の血小板面積は，高ALT症例がALT基準値内症例より小さかった(図4)(50,652±22,250 μm² vs. 69,203±16,033 μm²，P=0.1)．

(4)肝脾組織でのTGF-β1発現

対象の全症例で，肝および脾組織にTGF-β1の発現がみられた．対象の肝組織におけるTGF-β1発現は，線維性に拡大した門脈域および線維性隔壁に沿ってみられた(図5)．対象の脾組織におけるTGF-β1発現は，主に赤脾髄の脾洞および脾索を構成する細胞に，びまん性にみられた(図5)．

(5)脾臓内の巨核球とTGF-β1発現

CD41とTGF-β1の二重免疫組織化学では，対象

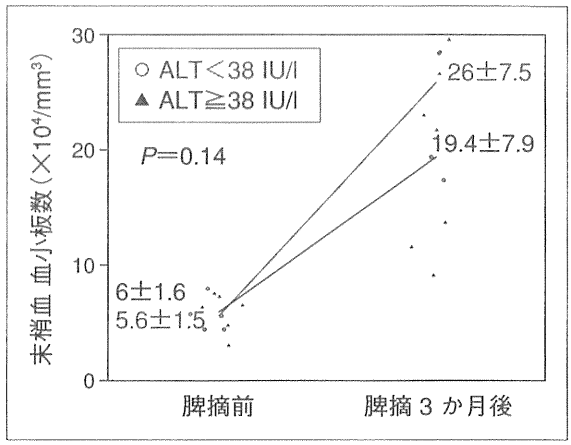

図1　脾摘前後での末梢血血小板数の推移
術前の血中ALT値が基準値(38 IU/l)以上であった7例(高ALT症例)は，ALT基準値内症例より脾摘3か月後の末梢血血小板数の改善が乏しい傾向にあった(末梢血血小板数，脾摘前→脾摘3か月後，6±2 mm³ → 19±8 mm³ vs. 6±1 mm³→26±8 mm³，P=0.14)．

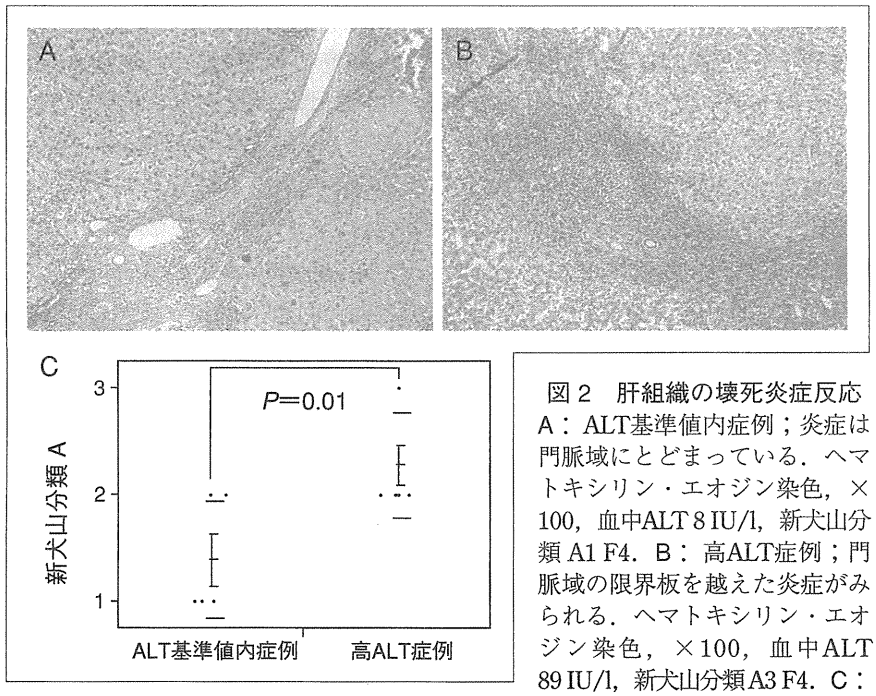

図2　肝組織の壊死炎症反応
A：ALT基準値内症例；炎症は門脈域にとどまっている．ヘマトキシリン・エオジン染色，×100，血中ALT 8 IU/l，新犬山分類 A1 F4．B：高ALT症例；門脈域の限界板を越えた炎症がみられる．ヘマトキシリン・エオジン染色，×100，血中ALT 89 IU/l，新犬山分類A3 F4．C：高ALT症例にみられる炎症はALT基準値内症例より有意に高度であった(新犬山分類 A，2±1 vs. 1±1，P=0.01)．

の脾組織において，赤脾髄の脾索にTGF-β1を発現した巨核球を認めた(図6)．脾組織内のTGF-β1陽性面積は，脾臓内に巨核球を認める症例が巨核球を認めない症例より有意に大きかった(図6)($P<0.01$)．

考　察

慢性肝炎・肝硬変の一般診療には，インター

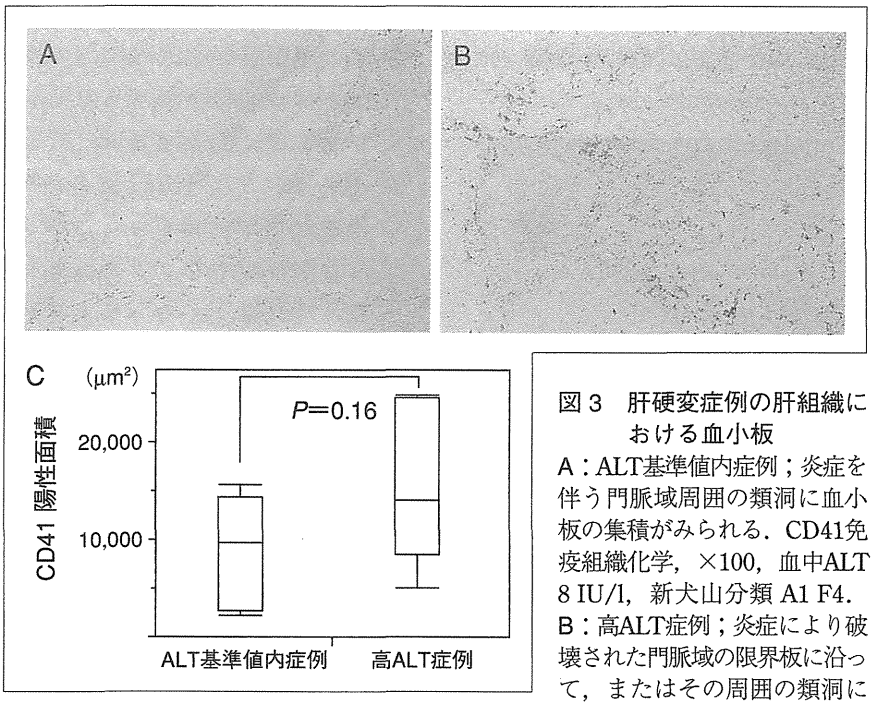

図3　肝硬変症例の肝組織における血小板
A：ALT基準値内症例；炎症を伴う門脈域周囲の類洞に血小板の集積がみられる．CD41免疫組織化学，×100，血中ALT 8 IU/l，新犬山分類 A1 F4．B：高ALT症例；炎症により破壊された門脈域の限界板に沿って，またはその周囲の類洞に血小板の集積がみられる．CD41免疫組織化学，×100，血中ALT 89 IU/l，新犬山分類 A3 F4．C：肝組織内の血小板面積は，高ALT症例がALT基準値内症例より大きい傾向にあった(15,217±8,058 μm² vs. 8,745±5,970 μm²，$P=0.16$)．

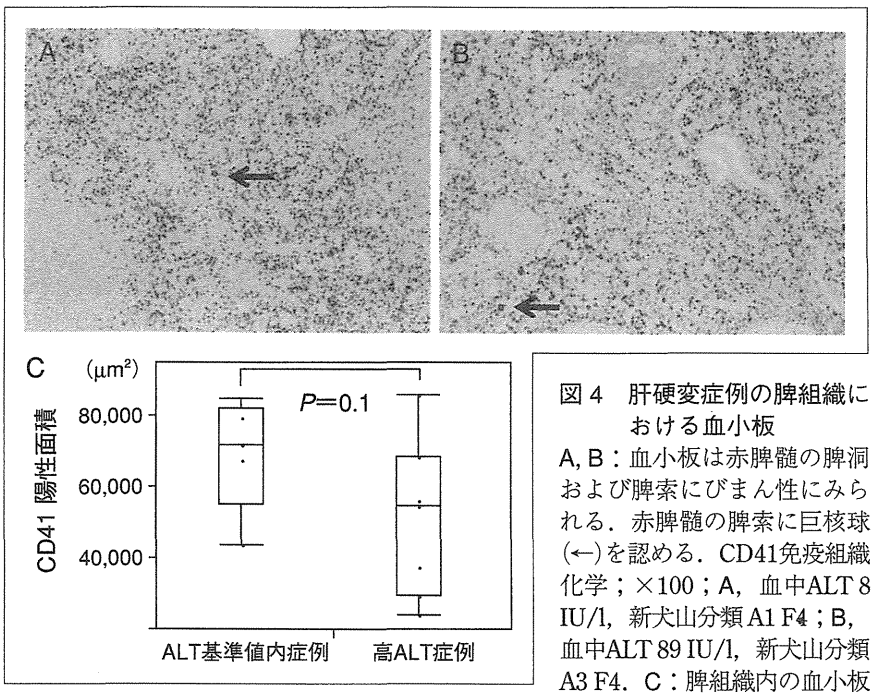

図4　肝硬変症例の脾組織における血小板
A, B：血小板は赤脾髄の脾洞および脾索にびまん性にみられる．赤脾髄の脾索に巨核球(←)を認める．CD41免疫組織化学；×100；A，血中ALT 8 IU/l，新犬山分類A1 F4；B，血中ALT 89 IU/l，新犬山分類A3 F4．C：脾組織内の血小板面積は，高ALT症例がALT基準値内症例より低い傾向にあった(50,652±22,250 μm² vs. 69,203±16,033 μm²，$P=0.1$)．

フェロン治療などの抗ウイルス治療あるいは胃食道静脈瘤や肝細胞癌に対する観血的治療が含まれ，慢性肝炎・肝硬変に伴う末梢血血小板減少は治療方針を左右する大きな要因となる．

本研究では，肝硬変における肝臓，脾臓への血小板の分布を病理組織学的に明らかにし，肝硬変に伴う末梢血血小板減少に対する脾摘の効果と肝臓への血小板集積について検討した．本研究で，対象の高ALT症例は，ALT基準値内症例より脾摘後の末梢血血小板数の改善が乏しかった．高ALT症例は，ALT基準値内症例より肝組織に高度の壊死炎症反応がみられ，肝組織内により多くの血小板を認めた．肝組織における血小板は炎症が強い門脈域周囲の類洞に集積がみられた．本研究の結果からは，肝臓の壊死炎症反応が高度な肝硬変症例は，肝臓に血小板がより多く集積するため，脾摘による末梢血血小板数改善の効果が減弱することが示唆された．

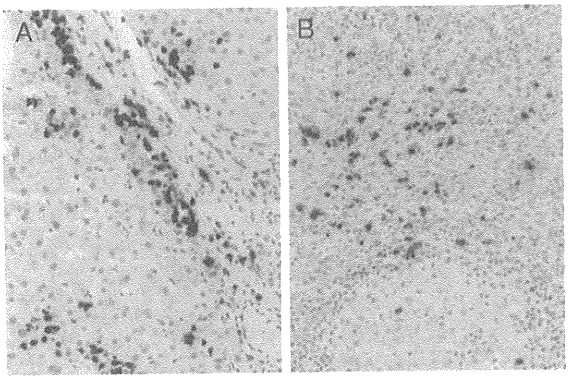

図5　肝硬変症例の肝脾組織におけるTGF-β1発現
A：肝組織；線維性に拡大した門脈域および線維性隔壁に沿ってTGF-β1の発現がみられる．TGF-β1免疫組織化学，×200．B：脾組織；主に赤脾髄の脾洞および脾索を構成する細胞に，TGF-β1の発現がびまん性にみられる．TGF-β1免疫組織化学，×200．

血管内において，血小板は血管内皮細胞が傷害を受けると，フォンヴィレブランド因子(von Willebrand factor；vWF)を介してコラーゲンなどの細胞外基質に接着し，偽足を伸展させ扁平に形態変化する．さらに，強固に粘着するため血小板の膜糖蛋白であるGP IIb/IIIa(integrin αIIbβ3)が活性化する[12]．肝組織においても血管内と同様に，類洞内皮細胞が傷害されると血小板が内皮細胞に粘着することが報告されている[13]．

血小板シンチグラフを用いた検討では，Kinuyaら[14]が，脾臓と肝臓に分布する血小板の比(spleen/

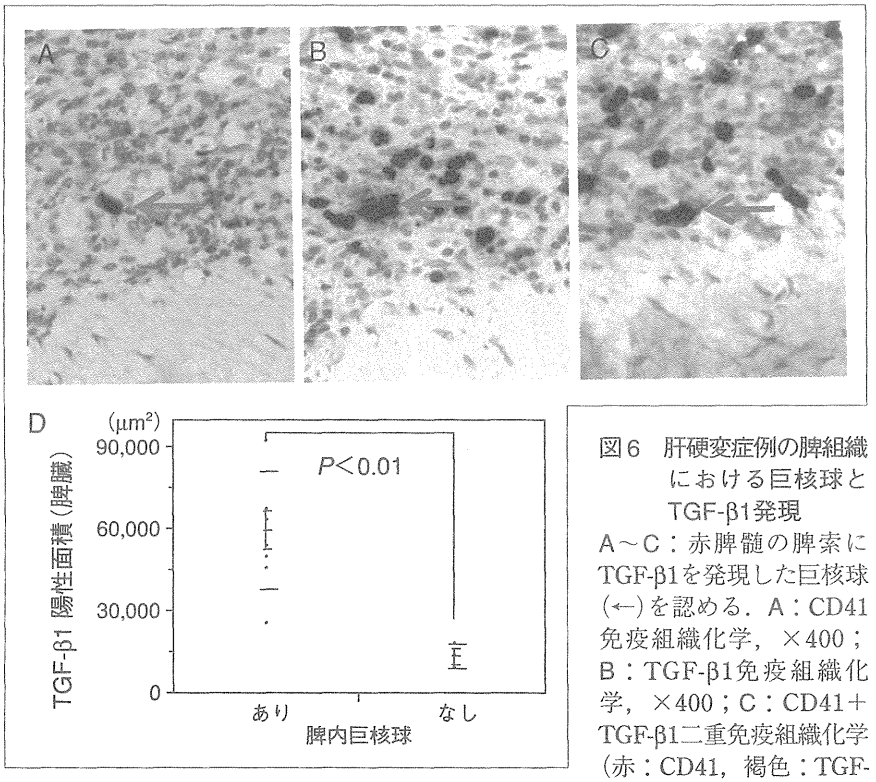

図6　肝硬変症例の脾組織における巨核球とTGF-β1発現
A～C：赤脾髄の脾索にTGF-β1を発現した巨核球(←)を認める．A：CD41免疫組織化学，×400；B：TGF-β1免疫組織化学，×400；C：CD41＋TGF-β1二重免疫組織化学(赤：CD41，褐色：TGF-β1)，×400．D：脾組織内のTGF-β1陽性面積は，脾臓内に巨核球を認める症例が巨核球を認めない症例より有意に大きかった($P<0.01$)．

liver ratio)が低い症例は，末梢血血小板減少症に対して脾摘を施行しても末梢血血小板数の回復が十分には得られなかったと報告している．末梢血血小板減少の要因として，肝臓への血小板集積は重要な病態である．

また今回の検討では対象の脾組織で，多くの症例に巨核球を認めた．巨核球にはTGF-β1の発現がみられ，巨核球を認める脾組織は巨核球を認めない脾組織よりTGF-β1の発現が高度であった．慢性肝炎において，TGF-β1は肝線維化に寄与する生理活性因子であることが報告されている[15)16)]．肝硬変では脾臓でのTGF-β1産生が増加し，脾臓で産生されたTGF-β1は門脈血を介して肝線維化に寄与すると報告されている[7)]．巨核球や血小板の内部には，さまざまな生理活性因子が包含されており，TGF-β1は巨核球や血小板に含まれる代表的な生理活性因子である[17)18)]．脾臓でのTGF-β1産生はマクロファージのかかわりが報告されているが，十分には明らかになっておらず，本研究の結果から脾臓でのTGF-β1産生に巨核球の関与も示唆された[7)8)]．

まとめ

肝臓への血小板集積が，肝硬変による末梢血血小板減少に対する脾摘の効果に関与するかを検討した．肝臓の壊死炎症反応が肝臓への血小板集積に寄与し，肝硬変による末梢血血小板減少に対する脾摘の効果を減弱させることが示唆された．肝脾組織内にみられる血小板，巨核球から，慢性肝炎に伴う末梢血血小板減少および肝線維化の治療につながる新しい見解を提案できる可能性があり，更なる検討が必要である．

文　献

1) Aster RH. Pooling of platelets in the spleen : role in the pathogenesis of "hypersplenic" thrombocytopenia. J Clin Invest 1966 ; 45 : 645.
2) Aoki Y, Hirai K, Tanikawa K. Mechanism of thrombocytopenia in liver cirrhosis : kinetics of indium-111 tropolone labelled platelets. Eur J Nucl Med 1993 ; 20 : 123.
3) Peck-Radosavljevic M. Thrombocytopenia in liver disease. Can J Gastroenterol 2000 ; 14 Suppl D : 60D.
4) Kondo R, Yano H, Nakashima O, et al. Accumulation of platelets in the liver may be an important contributory factor to thrombocytopenia and liver fibrosis in chronic hepatitis C. J Gastroenterol 2013 ; 48 : 526.
5) Kercher KW, Carbonell AM, Heniford BT, et al. Laparoscopic splenectomy reverses thrombocytopenia in patients with hepatitis C cirrhosis and portal hypertension. J Gastrointest Surg 2004 ; 8 : 120.
6) Sangro B, Bilbao I, Herrero I, et al. Partial splenic embolization for the treatment of hypersplenism in cirrhosis. Hepatology 1993 ; 18 : 309.
7) Akahoshi T, Hashizume M, Tanoue K, et al. Role of the spleen in liver fibrosis in rats may be mediated by transforming growth factor β-1. J Gastroenterol Hepatol 2002 ; 17 : 59.
8) Ueda S, Yamanoi A, Hishikawa Y, et al. Transforming growth factor β-1 released from the spleen exerts a growth inhibitory effect on liver regeneration in rats. Lab Invest 2003 ; 83 : 1595.
9) Morinaga A, Ogata T, Kage M, et al. Comparison of liver regeneration after a splenectomy and splenic artery ligation in a dimethylnitrosamine-induced cirrhotic rat model. HPB (Oxford) 2010 ; 12 : 22.
10) Nomura Y, Kage M, Ogata T, et al. Influence of splenectomy in patients with liver cirrhosis and hypersplenism. Hepatol Res 2013 Sep 3 [Epub ahead of print].
11) Duperray A, Troesch A, Berthier R, et al. Biosynthesis and assembly of platelet GPIIb-IIIa in human megakaryocytes : evidence that assembly between pro-GPIIb and GPIIIa is a prerequisite for expression of the complex on the cell surface. Blood 1989 ; 74 : 1603.
12) 冨山佳昭．先天性血小板機能異常症—受容体異常症．坂田洋一，小澤敬也・編．別冊・医学の歩み．血液疾患—state of arts．Ver. 3. 2005. p. 728.
13) Miyazawa Y, Tsutsui H, Mizuhara H, et al. Involvement of intrasinusoidal hemostasis in the development of concanavalin A-induced hepatic injury in mice. Hepatology 1998 ; 27 : 497.

14) Kinuya K, Matano S, Nakashima H, Taki S. Scintigraphic prediction of therapeutic outcomes of splenectomy in patients with thrombocytopenia. Ann Nucl Med 2003 ; 17 : 161.
15) Border WA, Noble NA. Transforming growth factor beta in tissue fibrosis. N Engl J Med 1994 ; 331 : 1286.
16) Sanderson N, Factor V, Nagy P, et al. Hepatic expression of mature transforming growth factor beta 1 in transgenic mice results in multiple tissue lesions. Proc Natl Acad Sci USA 1995 ; 92 : 2572.
17) Castro-Malaspina H. Pathogenesis of myelofibrosis : role of ineffective megakaryopoiesis and megakaryocyte components. Prog Clin Biol Res 1984 ; 154 : 427.
18) Chagraoui H, Komura E, Tulliez M, et al. Prominent role of TGF-β1 in thrombopoietin-induced myelofibrosis in mice. Blood 2002 ; 100 : 3495.

* * *